Earth Syst. Dynam. Discuss., 3, 1321–1345, 2012
www.earth-syst-dynam-discuss.net/3/1321/2012/
doi:10.5194/esdd-3-1321-2012

Earth System Dynamics Discussions

Climate change impact on available water resources obtained using multiple global climate and hydrology models

S. Hagemann[1], C. Chen[1], D. B. Clark[2], S. Folwell[2], S. N. Gosling[3], I. Haddeland[4], N. Hanasaki[5], J. Heinke[6], F. Ludwig[7], F. Voß[8], and A. J. Wiltshire[9]

[1]Max Planck Institute for Meteorology, Bundesstr. 53, 20146 Hamburg, Germany
[2]Center for Ecology and Hydrology, Wallingford, UK
[3]School of Geography, University of Nottingham, Nottingham, UK
[4]Norwegian Water Resources and Energy Directorate, Oslo, Norway
[5]National Institute for Environmental Studies, Tsukuba, Japan
[6]Potsdam Institute for Climate Impact Research, Potsdam, Germany
[7]Wageningen University and Research Centre, Wageningen, The Netherlands
[8]Center for Environmental Systems Research, University of Kassel, Kassel, Germany
[9]Met Office Hadley Centre, Exeter, UK

Received: 12 November 2012 – Accepted: 28 November 2012 – Published: 4 December 2012

Correspondence to: S. Hagemann (stefan.hagemann@zmaw.de)

Published by Copernicus Publications on behalf of the European Geosciences Union.

Abstract

Climate change is expected to alter the hydrological cycle resulting in large-scale impacts on water availability. However, future climate change impact assessments are highly uncertain. For the first time, multiple global climate (three) and hydrological models (eight) were used to systematically assess the hydrological response to climate change and project the future state of global water resources. The results show a large spread in projected changes in water resources within the climate–hydrology modelling chain for some regions. They clearly demonstrate that climate models are not the only source of uncertainty for hydrological change. But there are also areas showing a robust change signal, such as at high latitudes and in some mid-latitude regions, where the models agree on the sign of projected hydrological changes, indicative of higher confidence. In many catchments an increase of available water resources is expected but there are some severe decreases in central and Southern Europe, the Middle East, the Mississippi river basin, Southern Africa, Southern China and south eastern Australia.

1 Introduction

Global warming due to increased greenhouse gas emissions leads to changes in the distribution of water resources over many regions and the global and regional hydrological cycles have been greatly influenced by climate change in the past century (Brutsaert and Palange, 1998; Scanlon et al., 2007; Solomon et al., 2007). Following the greenhouse gas emission scenarios for the 21st century (Nakicenovic et al., 2000), climate change will cause increased temperatures and changes in precipitation. Future changes in rainfall however are highly uncertain and depend on which climate model is used. Hydrological models have been widely used for assessments of water resources, especially for studying the impacts of climate change. Many studies have tried to assess the impact of climate change on the past and future global water cycle. To cover

Discussion Paper | Discussion Paper | Discussion Paper | Discussion Paper |

ESDD

3, 1321–1345, 2012

Climate change impact on available water resources obtained

S. Hagemann et al.

part of the uncertainty in future climate change often multiple climate models are used but in most cases only one or two hydrological impact models are applied (Gosling and Arnell, 2011; Oki et al., 2003; Nijssen et al., 2001; Döll et al., 2003; Hagemann et al., 2011). Recent studies (Haddeland et al., 2011; Gosling et al., 2011), however, showed that differences between hydrological models are also a major source of uncertainty, and it was suggested that multiple impact models should be used for climate change impact studies (Haddeland et al., 2011). In the present study, climate projections from three state-of-the-art coupled atmosphere-ocean general circulation models (GCMs), eight global hydrology models (GHMs) and two emission scenarios are used to assess the response of the terrestrial hydrological cycle to climate change and subsequent changes in available water resources. In this respect, this is not only the first study to investigate future water resources using multiple GCMs and GHMs and emission scenarios, but it is also rigorous because eight GHMs were applied, which is by far the most applied in any global climate change impact study thus far. As GCM simulations are significantly affected by systematic errors, and results from a directly forced hydrological simulation will be unrealistic and of little use (Sharma et al., 2007; Hansen et al., 2006), bias-corrected GCM output was used to force the GHMs.

Section 2 describes the GCM-GHM modelling chain and the measures used to analyse the results. Mean changes in large-scale water fluxes and related uncertainties are presented in Sect. 3, where also a comparison to water fluxes obtained directly from the GCMs is included. The impact of climate change on the available water resources is estimated based on the multi-model ensemble results in Sect. 4. Finally, the results are summarized and discussed in Sect. 5, thereby also highlighting aspects of uncertainty introduced by GHMs.

Note that this study focuses on the impact of climate change alone on water fluxes and resources where direct human influences are not considered. However, land use and water use practices also play a role in the assessment whether and how strongly human societies are affected in regions with changing water resources. For an estimation of combined anthropogenic and climate change effects, water use and further

ESDD
3, 1321–1345, 2012

direct anthropogenic impacts on hydrology have to be taken into account which will be investigated by Haddeland et al. (2013).

2 Models and methods

2.1 Models

Three GCMs are used in this study to provide quantitative estimates of future climate projections following the IPCC emission scenarios A2 and B1 (Nakicenovic et al., 2000): ECHAM5/MPIOM (denoted as ECHAM5 henceforth) of the Max Planck Institute for Meteorology, LMDZ-4 of Institute Pierre Simon Laplace (denoted as IPSL henceforth) and CNRM-CM3 of Centre National de Recherches Météorologiques, Météo-France (denoted as CNRM henceforth). A statistical bias-correction method (Piani et al., 2010a,b) was applied to the GCM daily land precipitation and mean, minimum and maximum daily land temperatures. The bias-correction method is based on a fitted histogram equalization function. This function is defined daily, as opposed to earlier published versions in which they were derived yearly or seasonally at best, while conserving properties of robustness and eliminating unrealistic jumps at seasonal or monthly transitions. Bias-correction factors are derived from 1960 to 1999 from observed (Weedon et al., 2011) and simulated data and then applied to 1960–2100 simulations (Piani et al., 2010b). For details about the GCM simulations and the bias-corrected data, see Hagemann et al. (2011). Although bias correction of climate forcing fields has become a necessary step in climate impact simulations, many recent studies have identified limitations and pitfalls associated with this process (e.g. Haerter et al., 2011; Ehret et al., 2012). However, as stated by Piani and Haerter (2012) the used bias correction has been applied successfully to regional climate model output over Europe to examine the effects on both simulated climate and extreme hydrological events (Dosio and Paruolo, 2012; Rojas et al., 2011).

ESDD
3, 1321–1345, 2012

Eight GHMs (MPI-HM, LPJmL, WaterGAP, VIC, Mac-PDM.09, H08, GWAVA and JULES) were used to calculate historic and future water fluxes and simulate the land surface hydrology at a horizontal resolution of 0.5° (about 50 km grid spacing). For model characteristics and the physical processes represented, see Haddeland et al. (2011). This study focused on the impact of climate change on hydrology, and hence anthropogenic influences such as water withdrawals and reservoirs were not taken into account in the hydrological simulations.

2.2 Experimental setup and measures

To evaluate the projected hydrological cycle obtained from the multi-model ensemble, the ensemble means and the spread around these means due to different sources were calculated. For both emission scenarios, transient simulations from 1960–2100 were conducted by the GHMs. For the A2 scenario, simulations by all 8 GHMs forced by output from the 3 GCMs resulted in 24 different time series for each hydrological variable. For the B1 scenario, 18 simulations were obtained from 6 GHMs (excluding JULES and H08) forced by 3 GCMs. The ensemble mean of each hydrological variable was calculated for the control (1971–2000) and future (2071–2100) periods, and the changes are expressed for the future relative to the control period.

In this study, uncertainty is reflected by the spread of the model results due to the choice of the GCM (3), GHM (8) or emission scenario (2). For the first two, the spread is calculated from the normalized standard deviation (or coefficient of variation, CV) that is commonly used to express relative differences between models. Here, the spread due to the choice of the GCM is determined by taking the ensemble mean of the 8 GHM results for each GCM, and subsequently calculating the standard deviation among the 3 GCMs. The GHM spread is calculated correspondingly from the standard deviation of the GCM ensemble (3) means for each of the 8 GHMs. For the emissions, the scenario spread is represented by the differences between the ensemble mean results of the high emission scenario A2 and the lower emission scenario B1, obtained from those GHM simulations that were conducted for both scenarios ($6 \times 3 = 18$). As

ESDD
3, 1321–1345, 2012

this study focuses on changes in available water resources, associated changes in the main components of the terrestrial water balance are considered, i.e. precipitation (simulated by the GCMs), total runoff and evapotranspiration (simulated by the GHMs forced with bias-corrected GCM data).

3 Mean changes in large-scale water fluxes and related uncertainties

According to the results of the GCM A2 simulations, precipitation is projected to increase by the end of the 21st century across the higher latitude regions and in parts of the middle latitudes (Fig. 1a). Parts of the Middle East, the Mediterranean region, the southern parts of North America, Africa and Southern Australia will receive less precipitation. These future changes in precipitation are of a similar magnitude compared to the ensemble of 21 GCM results summarized in the 4th IPCC Assessment Report3. Noticeable uncertainties in the simulated precipitation change occur over northern Africa, the Indian monsoon region and Himalaya, some northern and western parts of South America, a small area in western Australia, the southern part of North America and over Greenland (Fig. 1b).

Water resources depend strongly on available runoff, which in the long term is constrained by incoming precipitation and outgoing evapotranspiration (ET). Runoff is projected to decrease over the eastern part of Australia, southern parts of Africa and United States, north east part of South America, south part of Europe, and large part of the Middle East (Fig. 2 – right column). Largely, the change pattern of runoff follows the ensemble mean change of precipitation (Fig. 1a). This behaviour is similar for the projected mean changes in ET (Fig. 2 – left column), with the noticeable exception that ET also increases in the northern high and mid-latitudes and extends further southwards into the transitional wet regions. This can be observed over south-eastern US, central Europe and eastern Asia.

Although for many large regions around the globe there is generally a large spread of absolute changes predicted by the different model simulations, many models agree in the sign of projected changes (Fig. 2c and d). For runoff, regions with relatively high mean changes are generally those regions where the majority of the 24 GCM-GHM model combinations agree on the sign of change. This indicates that the projected runoff changes expressed by the multi-model mean are robust within the used ensemble. The same applies for ET, except for relative changes in the Central Amazon and the very dry regions of Sahara and Southern Mexico where there is less agreement between the models.

For both runoff and ET we estimated whether the maximum spread in the projected changes originates from the choice of GCM, GHM or scenario. For ET (Fig. 3a), the uncertainty in the projected changes is largely dominated by the spread due to the choice of the GHM. Especially over high latitude regions, GHMs cause noticeable uncertainty patterns (Fig. 2g and h) where the spread originating from the GCMs is rather low (Fig. 2e and f). For runoff, the CV values representing the GCM spread are often comparable to the GHM spread even though the GCM spread is larger over many regions of the globe (Fig. 3b). The spread patterns associated with the runoff changes suggest that they are partially affected by the corresponding spreads in the ET changes. But the associated CV values are strongly reduced compared to the CV of the ET changes, especially over the mid- and low latitudes including central and Southern Europe. This means that on one hand the main spread in runoff changes originates from the choice of the GCM, which is especially imposed by the projected precipitation changes (Fig. 1). On the other hand, there are several areas where the runoff spread is dominated by the spread in ET changes that is largely induced by the GHMs, noticeably over the high northern latitudes.

In the A2 scenario, some high and mid latitude regions show more precipitation and runoff than with the B1 scenario (Fig. S1 in the Supplement). In most other areas, the projected changes are rather comparable. With regard to ET, most areas show larger values in the future period for the A2 scenario than for the B1 scenario, especially in the Amazon area. ET changes for A2 that are smaller than for B1 are projected over the western part of North America, southern part of South America and the Middle East.

ESDD
3, 1321–1345, 2012

This is an indication of a stronger drying of these regions with increased greenhouse gas concentrations. Noticeable spread due to choice of scenario largely occurs over areas where the projected ensemble mean A2 change is relatively small. In addition, larger runoff spreads occur over the high northern latitudes, Northern USA, some parts of South America and Africa that are comparable and partially larger (see Fig. 3) than those originating from the GCMs or GHMs. Over Africa, southern South America and northern USA, these uncertainties are induced by scenario differences in precipitation that are much larger than those originating from the choice of the GCM. Over the high latitudes, these seem to be related to scenario uncertainties in ET over these regions that are generally comparable to those rather low uncertainties originating from the GCMs or GHMs (Fig. S1 in the Supplement). In most other areas the scenario uncertainty is smaller than induced by the GCM or GHM.

Figure 4 sets the projected mean A2 changes in relation to the associated spreads over selected large-scale catchments that include the largest rivers on Earth as well as a few smaller catchments in Europe (Baltic Sea, Danube) and Australia (Murray). Following Hagemann et al. (2009), a projected change is considered robust if the change is larger than the maximum spread. Figure 4 shows that for many catchments the mean A2 change is robust compared to the different spreads, especially for runoff. For several catchments the direction of change is not robust, but relatively well constrained (larger than half of the maximum spread), i.e. Baltic Sea, Mississippi and Nile for runoff, and Amazon, Congo, Ganges/Brahmaputra and Nile for ET. Noticeably, the large GCM spread prohibits a constrained runoff change signal over the Ganges/Brahmaputra (runoff) and Parana (runoff and ET) catchments. Also, projected changes are not constrained for the Danube (ET) and Yangtze (runoff) due to low projected mean changes and large GHM spreads. Consistent with Fig. 3, the GHM spread of the ET changes is largest for most of the catchments (except for Mississippi and Parana), while for runoff the GCM spread prevails for 8 of the 12 catchments considered. But for the large area of the 6 largest Arctic rivers as well as for the catchments of Amur, Baltic Sea and Yangtze, the GHM spread is largest, demonstrating the impact of uncertainties in the

ESDD
3, 1321–1345, 2012

projected ET changes on the runoff changes over the high and some mid latitude regions. The scenario spread is generally the smallest spread, especially for runoff, and it is always smaller than the GHM spread, except for ET in the Murray catchment where it is largest. Catchments where the scenario spread is larger than the GCM spread usually comprise areas where the GCM spread is rather low.

It should be noted that only three GCMs were applied in this study, so that the uncertainty due to the choice of the GCM is likely somewhat underrepresented. However, the chosen GCMs belong to different model families and cover some range in projected precipitation change among the CMIP3 (Meehl et al., 2007; see also Sect. 5) ensemble (Mason and Knutti, 2011). The selection of GCMs for this study was imposed by the availability of climate model data necessary to force the GHMs. A respective analysis of the original GCM results over Europe was provided by Hagemann et al. (2008).

Comparison to direct GCM output

With regard to the projected changes in ET and runoff, it is interesting to compare the results from the GCM-GHM ensemble with the climate model output directly obtained from the three GCMs. The projected mean A2 changes and associated spreads among the 3 GCMs are shown in Fig. 5. The large-scale patterns of the mean changes are similar to the GCM-GHM ensemble (Fig. 2a and b), but the absolute intensity of changes is mostly lower in the direct GCM output. This is supported by Fig. 6 where the intensity of changes (decreases and increases) is compared. Here, the blue and red areas largely (larger changes in the GCM-GHM ensemble) exceed the turquoise and orange areas (larger changes in the original GCM output) for both ET and runoff. Areas (green), where the sign of change differs, are relatively scarce. In this respect, noticeable larger areas are seen for the runoff changes over Australia and east of the Caspian Sea. Considering average changes over large catchments (Fig. 4), it can be noted that the projected A2 changes from the original GCM output are often even weaker than the B1 changes from the GCM-GHM ensemble.

ESDD
3, 1321–1345, 2012

The spread patterns behave differently than the corresponding mean changes. For ET, the patterns of spread in the original GCM output (Fig. 5c) is rather similar to the spread due to the choice of the GCM in the GCM-GHM ensemble (Fig. 2e) over the southern hemisphere and the Tropics, but there are larger differences over the mid- and especially over the high northern latitudes. For runoff, both spreads (Figs. 5d and 2f)) show only some similarities over South America and Central Africa. Over most part of the globe, the spread in the original GCM output is larger than the GCM spread in the GCM-GHM ensemble (Fig. 6). The higher spread in the original GCM output seems to be a direct result of the GCM specific biases in precipitation and temperature. In the GCM-GHM ensemble, the bias correction is not only reducing the spread (per definition) in the GCM data for the control period, but also the spread in the climate change signal. Note that the absolute standard deviations of the original GCM output averaged over large catchments (Fig. 4) are partially smaller than the corresponding standard deviations in the GCM-GHM ensemble due to the choice of the GCM. But as the projected mean changes in the direct GCM output are mostly weaker than for the GCM-GHM ensemble (see above), the associated spreads represented by the CV (Fig. 5c and d) are often larger for the direct GCM output than their GCM-GHM counterparts (Fig. 6).

This means that even though the projected ET and runoff changes of the original GCM output are fully consistent with the other GCM variables, the associated spread and related uncertainties in these changes are larger than for the GCM-GHM ensemble where the consistency between variables is not necessarily the case due to the bias correction. Thus, the GCM specific biases in precipitation and temperature lead to higher spreads in the projected changes of terrestrial components of the hydrological cycle. Consequently, these results show another advantage of the chosen model setup compared to the direct use of GCM data for impact assessment, which can be regarded in the on-going discussion on pros and cons of bias correction (see Sect. 2.1).

ESDD
3, 1321–1345, 2012

4 Impact on the available water resources

Based on the results from the 8 GHMs and 3 GCMs, catchment based maps of changes in available water resources can identify areas that are vulnerable to projected climate change with regard to water availability. In this respect, available water resources are defined as the total annual runoff (R) minus the mean environmental water requirements. Using results of Smakhtin et al. (2004), environmental water requirements (EWR) for a catchment were defined as 30 % of the total annual runoff. Assuming EWR will not change significantly in the future, available water resources (ΔAW) can be estimated as:

$$\Delta\mathrm{AW} = ((R_{\mathrm{Scen}} - \mathrm{EWR}) - (R_{\mathrm{C20}} - \mathrm{EWR}))/(R_{\mathrm{C20}} - \mathrm{EWR}) = (R_{\mathrm{Scen}} - R_{\mathrm{C20}})/(R_{\mathrm{C20}} - \mathrm{EWR}).$$

Here, R_{C20} and R_{Scen} are the mean annual runoff for the current climate (1971–2000) and future scenario (2071–2100) periods, respectively, and $\mathrm{EWR} = 0.3\,R_{\mathrm{C20}}$.

Although for runoff there is large uncertainty induced by the choice of a GCM (see Figs. 2 and 3), most large catchments (e.g. Amazon, Parana, Nile, Congo, Ganges/Brahmaputra) show an increase in available water resources in the future (Fig. 7). There is some agreement between the 3 GCMs where the available water resources are expected to decrease considerably (more than 10 %). These regions comprise Central, Eastern and Southern Europe, the catchments of the Euphrates/Tigris in the Middle East, Mississippi in North America, Zhu Jiang in Southern China, Murray in SE Australia, and Okavango and Limpopo in Southern Africa. Here, the projections based on the different GCMs largely agree. As only three GCMs are considered, potential future significant reductions in available water resources based only on one of these GCMs cannot be neglected for this impact assessment. Examples of significant decreases are seen in the following large catchments for individual GCMs (Fig. 7): Parana (more than −50 % for IPSL) and Uruguay (more than −20 % for IPSL) in South America, Orange (more than −20 % for ECHAM) in South Africa, Sahel zone comprising Senegal, Niger, Volta and Chari (more than −50 % for IPSL) and Central and

ESDD
3, 1321–1345, 2012

Eastern Asia comprising the Ganges/Brahmaputra (more than −20 % for IPSL), Indus, Amudarja and Huang He (more than −10 % for ECHAM).

Climate change has been identified as a major influence on basin water balances. However, land use and water use practices also play a role in the assessment of whether and how strongly human societies are affected in those changing regions. The impact of reduced water availability on different regions also depends on the total water demand and during which season availability will change. These effects are necessary subjects for future studies.

5 Conclusions and discussion

The climate modelling community has a long history in systematic model intercomparison through the climate model intercomparison projects (CMIPs; Meehl et al., 2000). The results of CMIP3 (Meehl et al., 2007) are the basis for the future climate change projections presented in the IPCC 4th assessment report (Solomon et al., 2007). The results of CMIPs are also used in many climate change impact assessments to quantify the uncertainties originating from climate models and emission scenarios (Gosling et al., 2012; Osborne et al., 2012; Sperna Weiland et al., 2012). Most of the impact assessments however use only one impact model. For the first time, a multi-model ensemble comprising multiple global climate (3) and global hydrology models (8) was used to assess future large-scale changes in land surface water fluxes and available water resources. The results presented here clearly show that climate change impacts do not only depend on emission scenarios and climate models, but that different impact models give considerably different results. In some regions the spread of the impacts is higher than that of the climate models.

This ensemble of many different simulations formed the basis to compare the uncertainty in the projected changes originating from the choice of the GCM, the GHM and the emission scenario (B1 and A2). Here, we did not use the direct output of GCMs, but instead bias-corrected the GCM time series of precipitation and temperature on an individual basis. Thus, we essentially removed differences between GCMs in those time series in the baseline period, which correspondingly reduces the absolute spread of GCMs over many regions. Note that the relative values of projected hydrological change are very similar if also other GCM variables are bias-corrected (Haddeland et al., 2012). Future changes in runoff and evapotranspiration generally follow the projected changes in the bias-corrected GCM precipitation. These changes comprise projected increases over the high latitudes and some mid-latitude regions. Southern Europe, large parts of the Middle East, southern parts of Africa and the USA, eastern Australia and the north-eastern part of South America will likely experience decreased runoff in the future compared to the control period. Associated with this reduced runoff, a significant reduction in available water resources will occur in many catchments. For those regions, the projections based on the different GCMs largely agree. Moreover, when considering the large uncertainty associated with the choice of GCM, it is also possible that some regions might be affected by a significant future reduction in available water resources when this is projected only by one of the GCMs. Note that the direct use of GCM output is not recommended as biases in GCM temperature and precipitation lead to uncertainties in projected changes in terrestrial components of the hydrological cycle that are larger than in the model setup presented here. These also can lead to different climate change signals, which in the present study are generally weaker, but this may be a characteristic of the chosen 3 GCMs. Note that the usability of direct GCM output may change in the future as GCM developments are also being targeted at improving the water cycle and there are some studies in the literature implying there is useful information obtainable directly from GCMs (e.g. Falloon et al., 2011).

The results presented here show that the uncertainty in projected changes of land surface water fluxes due to the choice of the GHM cannot be neglected over many regions of the Earth. This uncertainly mainly arises from the different model formulations used to represent hydrological processes in the GHMs. Haddeland et al. (2011) found that significant differences between simulations by land surface models (LSMs;

ESDD
3, 1321–1345, 2012

models that calculate the land surface energy balance) and “pure” GHMs (without energy balance calculation) for the current climate are partly caused by the snow scheme applied. In that study, which included all the hydrological models that are included in this study, the physically-based energy balance approach used by LSMs generally resulted in lower snow water equivalent values than the conceptual degree-day approach used by most GHMs. Some differences in simulated runoff and evapotranspiration are explained by model parameterizations, such as the different treatment of soil moisture and evapotranspiration (Hagemann et al., 2011; Haddeland et al., 2011), although the processes included and parameterizations used are not distinct to either LSMs or pure GHMs. The present study indicates that large differences in the projected changes between the GHMs may be attributed to the different model formulations of evapotranspiration. This becomes especially obvious if the projected changes in evapotranspiration are considered for which the uncertainty related to the choice of the GHM is larger than due to the choice of the GCM over many regions. Uncertainties in projected evapotranspiration changes are generally shown to be due to the choice of the impact model whereas the choice of the climate model prevails for the future projections of runoff, except for those areas where the evapotranspiration is strongly affecting the future changes in runoff and, thus, the GHM uncertainty is more pronounced. Here, it has to be mentioned that the CO_2 stomata effect on evapotranspiration is neither accounted for by the GCMs nor by the GHMs except for 1 GHM (LPJmL). It has been shown that these impose a CO_2 physiological forcing on runoff (e.g. Betts et al., 2007), and that they are also important for large-scale precipitation over land so that similar GCM-GHM exercises (see below) with the forthcoming CMIP5 results are recommended to address associated uncertainties.

Future analyses of global climate change impacts to be used in for example the IPCC assessments should not be based on the output of single impact models. Well co-ordinated model intercomparison activities are not only needed for climate models but also for the important impacts. Our results show a clear need for intercomparison activities such as ISI-MIP (http://www.isi-mip.org), AgMIP (http://www.agmip.org/) and

ESDD
3, 1321–1345, 2012

WaterMIP (Haddeland et al., 2011; http://www.eu-watch.org/watermip). A major obstacle to the use by policy makers of the results of such model intercomparison projects is the large amount of data and scenarios produced by the different modelling exercises, which have to be reduced to a demonstrative and meaningful gist. Therefore, there is a need to develop tools and methods which allow for the quantification of uncertainty and assessment of robustness of climate change impacts using multi-model ensembles without generating too much data, and which may be used to demonstrate the associated results in a fairly simple way.

Supplementary material related to this article is available online at: http://www.earth-syst-dynam-discuss.net/3/1321/2012/esdd-3-1321-2012-supplement.pdf.

Acknowledgements. This study was supported by funding from the European Union within the WATCH project (contract No. 036946). Andrew Wiltshire was partly supported by the Joint DECC/Defra Met Office Hadley Centre Programme (GS01101). The authors would like to thank Tobias Stacke (MPI-M) for implementing several modifications into MPI-HM, Alexander Schröder (MPI-M) for some data processing and plotting, and Richard Gilham (UKMO) for data transfer and disaggregation work regarding JULES data. The GCM data were obtained from the CERA database at the German Climate Computing Center (DKRZ) in Hamburg. Additional data were thankfully provided by Nathalie Bertrand from IPSL.

References

Betts, R. A., Boucher, O., Collins, M., Cox, P. M., Falloon, P. D., Gedney, N., Hemming, D. L., Huntingford, C., Jones, C. D., Sexton, D. M., and Webb, M. J.: Projected increase in continental runoff due to plant responses to increasing carbon dioxide, Nature, 448, 1037–1041, 2007.

Brutsaert, W. and Parlange, M. B.: Hydrologic cycle explains the evaporation paradox, Nature, 396, p. 30, 1998.

ESDD

3, 1321–1345, 2012

Döll, P., Kaspar, F., and Lehner, B.: A global hydrological model for deriving water availability indicators: model tuning and validation, J. Hydrol., 270, 105–134, 2003.
Dosio, A. and Paruolo, P.: Bias correction of the ENSEMBLES high-resolution climate change projections for use by impact models: Evaluation on the present climate, J. Geophys. Res., 116, D16106, doi:10.1029/2011JD015934, 2011.
Ehret, U., Zehe, E., Wulfmeyer, V., Warrach-Sagi, K., and Liebert, J.: HESS Opinions "Should we apply bias correction to global and regional climate model data?", Hydrol. Earth Syst. Sci., 16, 3391–3404, doi:10.5194/hess-16-3391-2012, 2012.
Falloon, P., Betts, R., Wiltshire, A., Dankers, R., Mathison, C., McNeall, D., Bates, P., and Trigg, M.: Validation of river flows in HadGEM1 and HadCM3 with the TRIP river flow model, J. Hydrometeorol., 12, 1157–1180, 2011.
Gosling, S. N. and Arnell, N. W.: Simulating current global river runoff with a global hydrological model: model revisions, validation, and sensitivity analysis, Hydrol. Process., 25, 1129–1145, 2011.
Gosling, S. N., Taylor, R. G., Arnell, N. W., and Todd, M. C.: A comparative analysis of projected impacts of climate change on river runoff from global and catchment-scale hydrological models, Hydrol. Earth Syst. Sci., 15, 279–294, doi:10.5194/hess-15-279-2011, 2011.
Gosling, S. N., McGregor, G. R., and Lowe, J. A.: The benefits of quantifying climate model uncertainty in climate change impacts assessment: an example with heat-related mortality change estimates, Climatic Change, 112, 217–231, doi:10.1007/s10584-011-0211-9, 2012.
Haddeland, I., Clark, D. B., Franssen, W., Ludwig, F., Voß, F., Arnell, N. W., Bertrand, N., Best, M., Folwell, S., Gerten, D., Gomes, S., Gosling, S. N., Hagemann, S., Hanasaki, N., Harding, R., Heinke, J., Kabat, P., Koirala, S., Oki, T., Polcher, J., Stacke, T., Viterbo, P., Weedon, G. P., and Yeh, P.: Multi-model estimate of the global terrestrial water balance: setup and first results, J. Hydrometeorol., 12, 869–884, doi:10.1175/2011JHM1324.1, 2011.
Haddeland, I., Heinke, J., Voß, F., Eisner, S., Chen, C., Hagemann, S., and Ludwig, F.: Effects of climate model radiation, humidity and wind estimates on hydrological simulations, Hydrol. Earth Syst. Sci., 16, 305–318, doi:10.5194/hess-16-305-2012, 2012.
Haddeland, I., Biemans, H., Eisner, S., Fekete, B., Flörke, M., Hanasaki, N., Heinke, J., Ludwig, F., Schewe, J., Stacke, T., Wada, Y., and Wisser, D.: A global multi-model view on water balance alterations caused by human interventions versus climate change, to be submitted to P. Natl. Acad. Sci. in January 2013.

ESDD
3, 1321–1345, 2012

Haerter, J. O., Hagemann, S., Moseley, C., and Piani, C.: Climate model bias correction and the role of timescales, Hydrol. Earth Syst. Sci., 15, 1065–1079, doi:10.5194/hess-15-1065-2011, 2011.

Hagemann, S., Berg, P., Christensen, J. H., and Haerter, J.O.: Analysis of existing climate model results over Europe, WATCH Technical Rep. 7, http://www.eu-watch.org, European Union project (FP6) WATCH, 2008.

Hagemann, S., Göttel, H., Jacob, D., Lorenz, P., and Roeckner, E.: Improved regional scale processes reflected in projected hydrological changes over large European catchments, Clim. Dynam., 32, 767–781, doi:10.1007/s00382-008-0403-9, 2009.

Hagemann, S., Chen, C., Haerter, J. O., Gerten, D., Heinke, J., and Piani, C.: Impact of a statistical bias correction on the projected hydrological changes obtained from three GCMs and two hydrology models, J. Hydrometeorol., 12, 556–578, doi:10.1175/2011JHM1336.1, 2011.

Hansen, J. W., Challinor, A., Ines, A., Wheeler, T., and Moronet, V.: Translating forecasts into agricultural terms: advances and challenges, Climate Res., 33, 27–41, 2006.

Masson, D. and Knutti, R.: Climate model genealogy, Geophys. Res. Lett., 38, L08703, doi:10.1029/2011GL046864, 2011.

Meehl, G. A., Boer, G. J., Covey, C., Latif, M., and Stouffer, R. J.: The Coupled Model Intercomparison Project (CMIP), B. Am. Meteorol. Soc., 81, 313–318, 2000.

Meehl, G. A., Covey, C., Delworth, T., Latif, M., McAvaney, B., Mitchell, J. F. B., Stouffer, R. J., and Taylor, K. E.: The WCRP CMIP3 multi-model dataset: A new era in climate change research, B. Am. Meteorol. Soc., 88, 1383–1394, 2007.

Nakicenovic, N., Alcamo, J., Davis, G., de Vries, B., Fenhann, J., Gaffin, S., Gregory, K., Grübler, A., Jung, T. Y., Kram, T., La Rovere, E. L., Michaelis, L., Mori, S., Morita, T., Pepper, W., Pitcher, H., Price, L., Raihi, K., Roehrl, A., Rogner, H.-H., Sankovski, A., Schlesinger, M., Shukla, P., Smith, S., Swart, R., van Rooijen, S., Victor, N., and Dadi, Z.: IPCC Special Report on Emissions Scenarios. Cambridge University Press, Cambridge, UK and New York, NY, USA, 2000.

Nijssen, B., O'Donnell, G. M., Hamlet, A. F., and Lettenmaier, D. P.: Hydrologic sensitivity of global rivers to climatic change, Climatic Change, 50, 143–175, 2001.

Oki, T., Agata, Y., Kanae, S., Saruhashil, T., and Musiake, K.: Global water resources assessment under climatic change in 2050 using TRIP. Water Resources Systems – Water

ESDD
3, 1321–1345, 2012

availability and global change, IÂHS Publ. 280, Proceedings of symposium HS02a held during IUGG2003 at Sapporo, July 2003.
Osborne, T., Rose, G., and Wheeler, T.: Variation in the global-scale impacts of climate change on crop productivity due to climate model uncertainty and adaptation, Agr. Forest. Meteorol., doi:10.1016/j.agrformet.2012.07.006, in press, 2012.
Piani, C. and Haerter, J. O.: Two dimensional bias correction of temperature and precipitation copulas in climate models, Geophys. Res. Lett., doi:10.1029/2012GL053839, in press, 2012.
Piani, C., Haerter, J. O., and Coppola, E.: Statistical bias correction for daily precipitation in regional climate models over Europe, Theor. Appl. Climatol., 99, 187–192, 2010a.
Piani, C., Weedon, G. P., Best, M., Gomes, S., Viterbo, P., Hagemann, S., and Haerter, J. O.: Statistical bias correction of global simulated daily precipitation and temperature for the application of hydrological models, J. Hydrol., 395, 199–215, 2010b.
Rojas, R., Feyen, L., Dosio, A., and Bavera, D.: Improving pan-European hydrological simulation of extreme events through statistical bias correction of RCM-driven climate simulations, Hydrol. Earth Syst. Sci., 15, 2599–2620, doi:10.5194/hess-15-2599-2011, 2011.
Scanlon, T. S., Caylor, K. K., Levin, S. A., and Rodriguez-Iturbe, I.: Positive feedbacks promote power-law clustering of Kalahari vegetation, Nature, 449, 209–212, 2007.
Sharma, D., Das Gupta, A., and Babel, M. S.: Spatial disaggregation of bias-corrected GCM precipitation for improved hydrologic simulation: Ping River Basin, Thailand, Hydrol. Earth Syst. Sci., 11, 1373–1390, doi:10.5194/hess-11-1373-2007, 2007.
Smakhtin, V., Revenga, C., and Döll, P.: A Pilot Global assessment of environmental water requirements and scarcity, Water Int. 29, 307–317, 2004.
Solomon, S., Qin, D., Manning, M., Marquis, M., Averyt, K., Tignor, M. M. B., Miller Jr., H. L., and Chen, Z. (Eds.): Climate Change 2007: The Physical Science Basis, Cambridge University Press, 996 pp., 2007.
Sperna Weiland, F. C., van Beek, L. P. H., Kwadijk, J. C. J., and Bierkens, M. F. P.: Global patterns of change in discharge regimes for 2100, Hydrol. Earth Syst. Sci., 16, 1047–1062, doi:10.5194/hess-16-1047-2012, 2012.
Weedon, G. P., Gomes, S., Viterbo, P., Shuttleworth, W. J., Blyth, E., Österle, H., Adam, J. C., Bellouin, N., Boucher, O., and Best, M.: Creation of the WATCH forcing data and its use to assess global and regional reference crop evaporation over land during the twentieth century, J. Hydrometeorol., 12, 823–848, doi:10.1175/2011JHM1369.1, 2011.

ESDD
3, 1321–1345, 2012

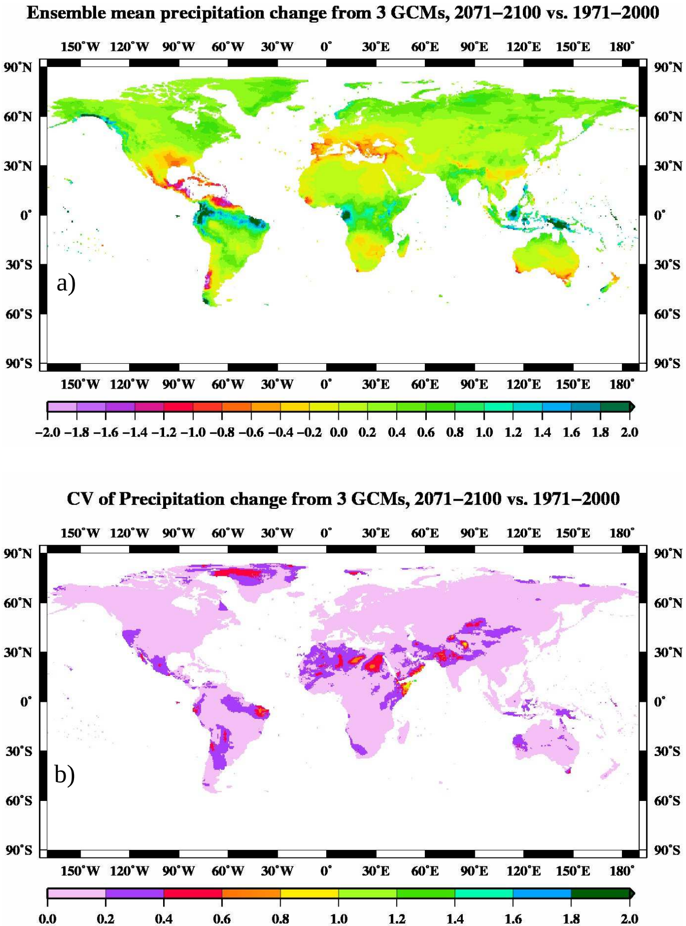

Fig. 1. Annual ensemble mean changes in precipitation [mm day^{-1}] projected by the three GCMs following the A2 scenario for 2071–2100 compared to 1971–2000 **(a)** and the CV of these changes from the three GCMs **(b)**.

ESDD
3, 1321–1345, 2012

Title Page
Abstract | Introduction
Conclusions | References
Tables | Figures
◀| |▶
◀ ▶
Back | Close
Full Screen / Esc
Printer-friendly Version
Interactive Discussion

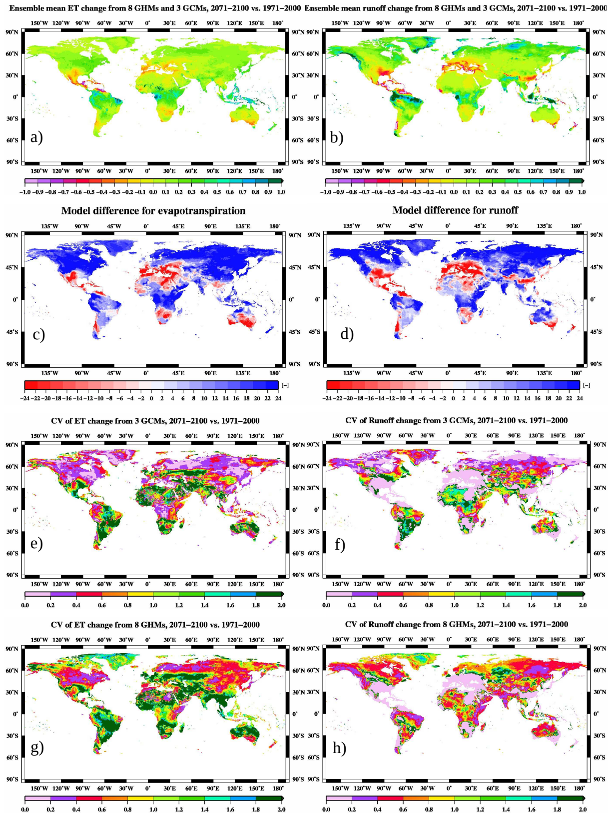

Fig. 2. Ensemble mean results for evapotranspiration (left column) and runoff (right column) from 24 simulations (8 GHMs using output from 3 GCMs): Mean future changes [mm day^{-1}] following the A2 scenario for 2071–2100 compared to 1971–2000 **(a, b)**, Number of simulations showing a positive change minus the number showing a negative change **(c, d)**, CV of these changes from 3 GCMs **(e, f)** and CV from 8 GHMs **(g, h)**.

ESDD
3, 1321–1345, 2012

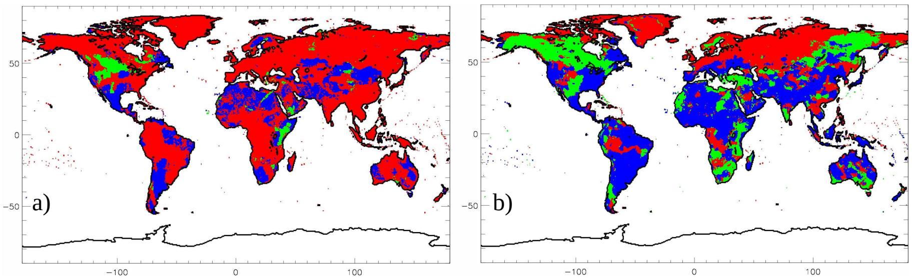

Fig. 3. Areas where the maximum spread in projected evapotranspiration **(a)** and runoff **(b)** changes (2071–2100 compared to 1971–2000) is due to the choice of the GCM (blue), GHM (red) or scenario (green).

ESDD
3, 1321–1345, 2012

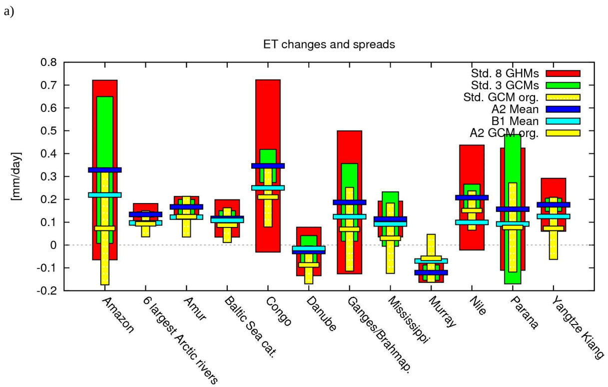

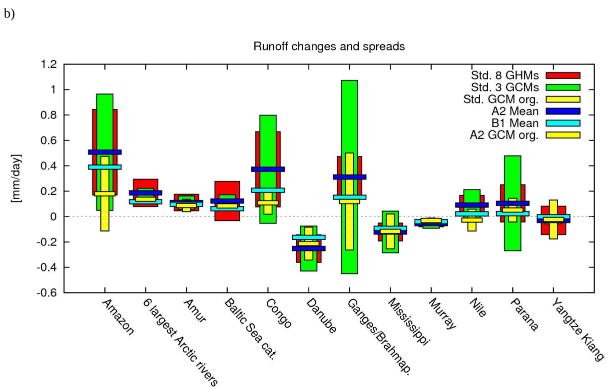

Fig. 4. Mean projected A2 and B1 changes (2071–2100 compared to 1971–2000) in evapotranspiration **(a)** and runoff **(b)** and associated spreads (Std. = standard deviation) due to the choice of the GCM (Std. 3 GCMs) and GHM (Std. 8 GHMs) around the A2 mean over selected large catchments. The mean A2 change and spread obtained directly from the three original GCM output are also shown (A2 GCM org., Std. GCM org.). The 6 largest Arctic rivers comprise the catchments of Mackenzie, Northern Dvina, Yenisei, Ob, Lena and Kolyma.

ESDD
3, 1321–1345, 2012

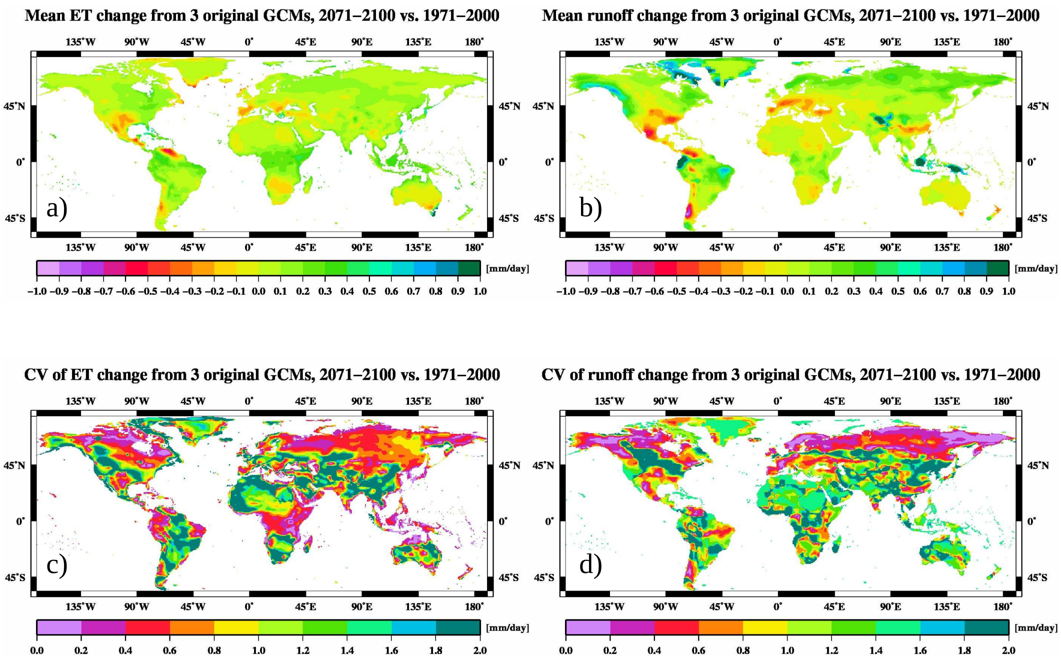

Fig. 5. Results obtained directly from the output of the 3 GCMs for evapotranspiration (left column) and runoff (right column): Mean future changes [mm day^{-1}] following the A2 scenario for 2071–2100 compared to 1971–2000 **(a, b)**, and the CV of these changes from the 3 GCMs **(c, d)**.

ESDD
3, 1321–1345, 2012

Climate change impact on available water resources obtained

S. Hagemann et al.

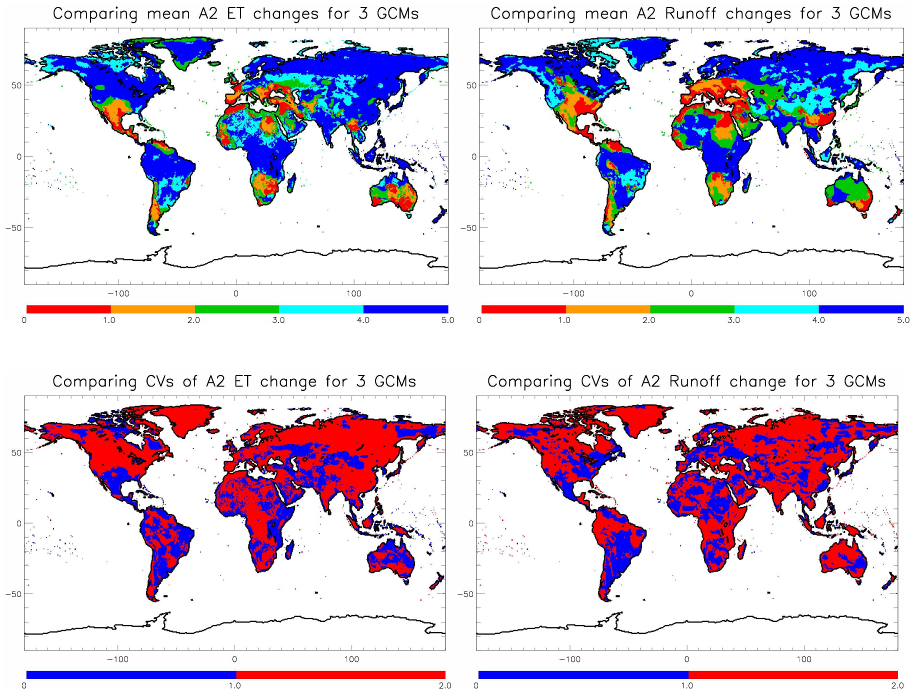

Fig. 6. Comparison of the projected mean A2 changes (2071–2100 compared to 1971–2000; upper panels) and the associated spreads due to the choice of the GCM for evapotranspiration (left column) and runoff (right column). In the upper panels, areas are indicated where the projected decreases and increases are larger in the GCM-GHM ensemble (red and blue, respectively) or for the original GCM output (orange and turquoise, respectively), as well as areas where the sign of projected change differs between them (green). In the lower panels, areas are indicated where the CV is larger for the GCM-GHM ensemble (blue) or for the original GCM output (red).

ESDD
3, 1321–1345, 2012

Climate change impact on available water resources obtained

S. Hagemann et al.

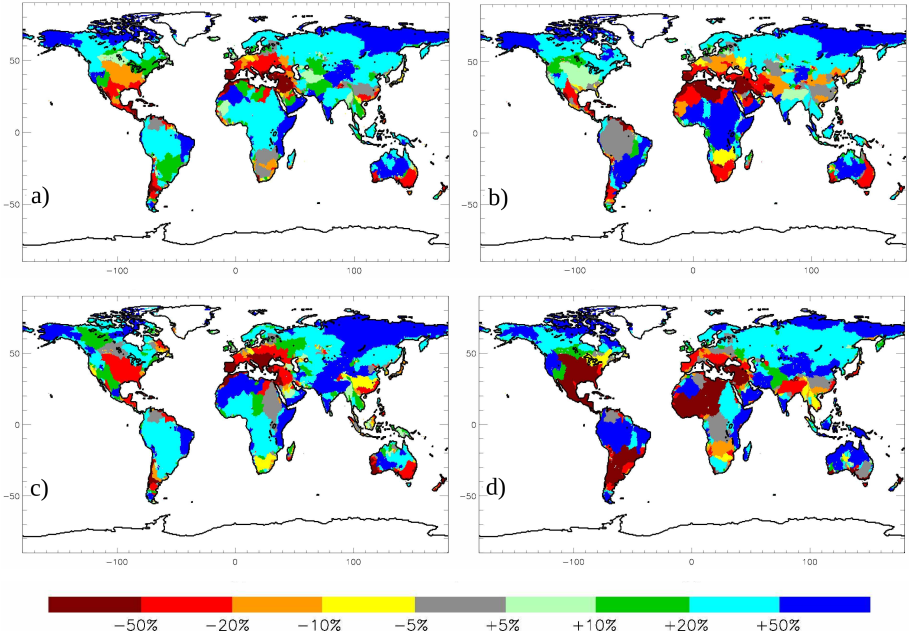

Fig. 7. A2 changes (2071–2100 compared to 1971–2000) in available water resources projected by the 8 GHM ensemble averaged for all 3 GCMs **(a)**, ECHAM **(b)**, CNRM **(c)** and IPSL **(d)**.

ESDD

3, 1321–1345, 2012